THE JOURNAL OF PHYSICAL CHEMISTRY A

Article

pubs.acs.org/JPCA

Effect of Curvature on Carbon Chemical Shielding in Extended Carbon Systems

Leah B. Casabianca*

Department of Chemistry, Clemson University, Clemson, South Carolina 29634-0973, United States

ABSTRACT: The effect of curvature on the chemical shielding of carbons in curved polycyclic aromatic hydrocarbons has been systematically studied by examining structures analogous to the circumcoronene molecule with different degrees of curvature. We attempt to eliminate effects from Knight shifts in carbon nanotubes, differing ring currents from five-membered rings, and edge effects in finite nanotube models in order to separate out the change in shielding that is due to curvature alone. Using curved structures derived from geometry-optimized structures of carbon nanotubes, we calculate the carbon chemical shielding tensor for carbons in the central aromatic ring as well as the Nucleus Independent Chemical Shift (NICS) on the convex and concave side of each structure. All three tensor components become less shielded with increasing curvature of the system, with the σ_{33} component radial to the curve experiencing the greatest change. The NICS values are influenced by both the decrease in aromaticity as the structure is curved as well as geometric effects that bring the outside rings closer to the central aromatic ring.

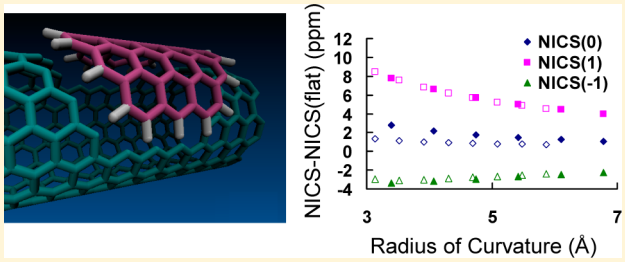

INTRODUCTION

Curved and bowl-shaped polycyclic aromatic hydrocarbons (PAH's) have received interest as models for fragments of curved fullerenes, and for their enhanced reactivity at central carbons as compared to flat PAH's.[1] Nanoporous carbon most likely contains a significant fraction of curved carbon structures, in addition to flat graphene-like sheets.[2−4] Fullerenes and carbon nanotubes are curved aromatic structures with interesting mechanical and electrical properties[5,6] leading to various potential applications. Bowl-shaped molecules and fullerene fragments, such as corannulene[7] and sumanene,[8] have been synthesized as well. Corannulene contains a central five-membered ring surrounded by six benzene rings. The central five-membered ring in corannulene introduces curvature into the aromatic structure. Sumanene is a bowl-shaped aromatic structure that forms the end-cap of the fullerene C_{60}. The structures of corannulene, sumanene, and the flat analogous molecule coronene are shown in Figure 1.

Carbon nanotubes[9] can be thought of as a rolled-up graphene sheets. The structure of a specific single-walled nanotube is described by two numbers (n,m) which indicate the number of a_1 and a_2 unit vectors in graphene, respectively, that make up the circumference of the nanotube. These numbers n and m determine the properties of the nanotube. Nanotubes with $(n,0)$ are called zigzag nanotubes and nanotubes with (n,n) are called armchair nanotubes. Other combinations of arbitrary n and m result in chiral nanotubes. Armchair nanotubes are always metallic, and zigzag nanotubes are semiconducting. Zigzag nanotubes for which n is a multiple of three are semiconducting with a vanishing band gap.[10]

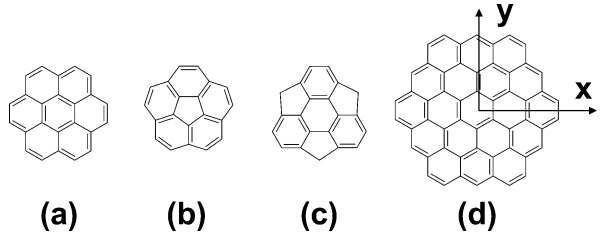

Figure 1. Structure of (a) coronene, (b) corannulene, (c) sumanene, and (d) circumcoronene.

Curved structures containing aromatic carbon rings have been studied by Nuclear Magnetic Resonance (NMR) both experimentally and theoretically.[11−15] Experiments indicate that carbons in curved structures are generally less shielded than carbons in the corresponding flat structures. For example, the central carbons in coronene have chemical shift tensor components of $\delta_{11} = \delta_{22} = 199$ ppm, $\delta_{33} = -38$ ppm, and $\delta_{iso} = 120$ ppm, while the central carbons in corannulene have shifts of $\delta_{11} = 224$ ppm, $\delta_{22} = 177$ ppm, $\delta_{33} = 6$ ppm, and $\delta_{iso} = 136$ ppm.[11] The two nonequivalent central carbons in sumanene have chemical shift tensor components of $\delta_{11} =$ 227.2 and 231.7 ppm, $\delta_{22} = 178.9$ and 181.3 ppm, $\delta_{33} = 29.2$ and 25.7 ppm, and $\delta_{iso} = 145.1$ and 146.2 ppm.[12]

The difficulty in comparing chemical shifts in flat and curved structures is that the result will depend on the models chosen for the flat and curved structures. For example, curved corannulene and sumanene contain one or more five-membered rings while planar coronene consists of only six-membered rings. According to the current density maps

Received: June 2, 2016
Revised: August 16, 2016
Published: August 26, 2016

DOI: 10.1021/acs.jpca.6b05560
J. Phys. Chem. A 2016, 120, 7011−7019

calculated by Fowler and co-workers, changing the number of carbon atoms in a polycyclic system will influence the magnetic properties of the system. Coronene and corannulene both have a diatropic ring current on the outer ring of carbon atoms, and a paratropic current on the central carbon ring. In coronene, the diatropic current is larger, whereas in corannulene the central paratropic current is stronger.[16] In contrast, benzene and circumcoronene experience a diatropic ring current on the central carbon ring.[16,17] Thus, the chemical shift differences between coronene and corannulene, for example, will be influenced by both the presence of curvature in corannulene and the differing magnetic properties of the two compounds. As another example of the choice of model influencing the magnetic properties of curved structures, Martín-Martínez et al.[18] performed calculations that indicate that edge effects in finite nanotubes (the length of the nanotube when modeling finite-length tubes) have an influence on the magnetic properties of the nanotube.

One example of a system in which curved and flat structures with the same number of carbons can be compared is cyclophanes, structures containing aromatic ring systems with cyclic aliphatic chains connecting the ends of the aromatic system. The cyclic aliphatic chains constrain the aromatic system, introducing curvature. Halling et al.[13] have used FIREMAT experiments to measure the chemical shift tensor components in [2.2]paracyclophane and 1,8-dioxa[8](2,7)-pyrenophane. The chemical shift tensor components for the central carbons in the latter are δ_{11} = 211.9 ppm, δ_{22} = 171.6 ppm, δ_{33} = 0.8 ppm, and δ_{iso} = 128.1 ppm. In comparison, shift tensor components for the central carbons in flat pyrene are δ_{11} = 197 ppm, δ_{22} = 191 ppm, δ_{33} = −18 ppm, and δ_{iso} = 123.3 ppm.[19] Comparing chemical shifts in cyclophanes with a flat polycyclic aromatic carbon analog also introduces difficulties. The aliphatic chain constrains the aromatic ring to only one degree of curvature, and the presence of substituents and crystal packing effects will also contribute to changes in chemical shifts. These studies inspired us to carry out a systematic study of the change in carbon chemical shift in polycyclic aromatic structure as the degree of curvature of the structure increases.

In addition to the chemical shift of the carbons themselves, another important parameter related to aromatic hydrocarbons is the Nucleus Independent Chemical Shift[20] (NICS) in, above, or below the hydrocarbon plane. NICS is the chemical shift that is felt by a neutron or ghost atom at any position in space. NICS calculated at a specific point in space can be used as a measure of the shielding experienced by a nucleus located at that point that is due to ring current effects from nearby aromatic rings.[21] NICSs calculated at the center or 1 Å above an aromatic ring have also been suggested as a measure of aromaticity,[20,22] although a more rigorous measure of aromaticity is obtained by calculating the full current density map.[23] NICS values have been calculated at positions inside[24−26] and outside[24] carbon nanotubes, in bowl-shaped polycyclic aromatic hydrocarbons,[27] and at the concave and convex faces of corannulene[2] and sumanene.[28]

In this work, we systematically examine the effect of curvature on chemical shielding in the absence of other effects. In order to remove edge effects, effects from differing ring current densities due to different number of carbon atoms, and Knight shifts caused by vanishing band gaps in certain families of carbon nanotubes,[29] we compare flat and curved structures with the same number of carbon atoms. We do this by examining the chemical shielding of carbons in circumcoronene, a 54-carbon polycyclic aromatic hydrocarbon shown in Figure 1d. We examine both the flat circumcoronene structure as well as circumcoronene-like structures in which curvature has been introduced by cutting a 54-carbon fragment from an optimized nanotube structure and passivating the dangling bonds with hydrogens. This allows us to determine the magnitude of the change in shielding that comes from curvature alone. Curvature was introduced in two mutually perpendicular directions by considering structures cut from $(n,0)$ and (n,n) nanotubes. We have investigated both changes to the chemical shielding tensor of the carbons themselves as well as the NICS on the concave and convex faces of the curved structures. The results presented here will be important in understanding chemical shielding, and by extension experimentally measured chemical shifts, of carbons in and near curved structures such as curved graphene fragments, mesoporous carbon materials, nanotubes, and fullerenes.

COMPUTATIONAL METHODS

Nanotubes were generated using the nanotube builder extension in Visual Molecular Dynamics (VMD).[30] A unit cell was created and optimized with periodic boundary conditions in Gaussian 09[31] using the HSEh1pbe functional[32−34] and a 6-31G basis set.[35] A 54-carbon fragment was then cut from each nanotube and passivated with hydrogen atoms, as shown in Figure 2. The positions of the hydrogen

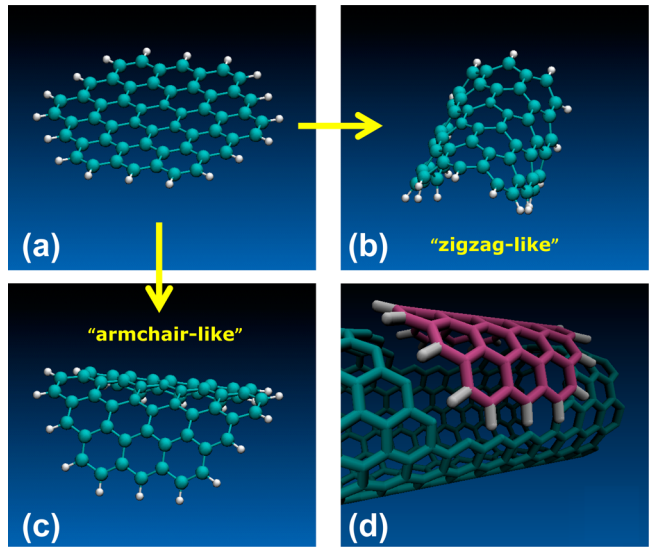

Figure 2. Generation of the curved model structures. A flat circumcoronene molecule (a) can be curved in either of two mutually perpendicular directions in order to form zigzag-like (b) or armchair-like (c) curved 54-carbon structures. (d) Illustration of how a curved structure is formed by cutting 54 carbons from an (8,8) carbon nanotube and passivating the edges with hydrogen atoms.

atoms were then optimized at the B3LYP/6-31G level of theory[35−37] while holding the positions of the carbon atoms fixed to maintain the intended curvature. Chemical shieldings were calculated for these curved structures using the B3LYP functional and a 6-311G basis set.[38] NICSs were calculated by placing ghost atoms at the center of the central carbon ring and on a line normal to the plane containing this ring every 0.25 Å for a total distance of 10 Å. Due to the curvature, the six central carbon atoms do not remain coplanar, so for the definition of the plane containing the central carbon ring, the four carbons

DOI: 10.1021/acs.jpca.6b05560
J. Phys. Chem. A 2016, 120, 7011−7019

Table 1. Calculated Chemical Shielding and Experimental Chemical Shift Tensor Components in Some Flat and Curved Structures (ppm)

	σ(11)	σ(22)	σ(33)	σ(iso)	δ(11)	δ(22)	δ(33)	δ(iso)
corannulene[a]								
hub	−36.7	10.7	170.9	48.3	224	177	6	136
rim	−29.5	−4.0	185.9	50.8	214	189	−10	131
protonated	−40.1	43.9	161.7	55.2	215	145	17	126
coronene[a]								
hub	−12.0	−1.2	196.3	61.0	199	199	−38	120
rim	−16.0	−11.8	190.5	54.2	204	193	−28	123
protonated	−41.5	52.6	161.5	57.5	225	137	7	123
sumanene[b]								
1,4,7	112.6	150.6	162.5	141.9	57.3	38.6	30.1	42.0
2,5,8	−33.4	44.1	166.9	59.2	207.3	143.0	16.6	122.3
3,6,9	−33.4	44.1	166.9	59.2	210.3	148.9	15.0	124.7
1a,4a,7a	−56.8	−0.5	149.2	30.6	231.6	178.0	32.8	147.5
3a,6a,9a	−56.8	−0.5	149.2	30.6	237.9	177.7	29.7	148.4
1b,4b,7b	−48.1	1.5	150.8	34.7	227.2	178.9	29.2	145.1
3b,6b,9b	−48.1	1.5	150.8	34.7	231.7	181.3	25.7	146.2
pyrene[c]								
C1	−38.6	49.6	164.9	58.6	212.0	141.0	21.0	124.7
C2	−52.9	47.0	178.3	57.5	226.0	140.0	4.0	123.3
C4=C10	−44.4	55.2	157.1	55.9	222.0	136.0	21.0	126.3
C3a	−29.6	−4.0	188.6	51.7	213.0	187.0	−7.0	131.0
C10b	−12.0	−7.9	195.8	58.6	197.0	191.0	−18.0	123.3

[a]Experimental data from ref 11. [b]Experimental data from ref 12. [c]Experimental data from ref 19.

that do remain coplanar were used. NICS are reported as the opposite of the calculated shielding, in order to convert shielding to chemical shift.

For comparison with a flat structure, a 54-carbon fragment was cut from the structure of graphene optimized using the HSEh1pbe functional[32−34] and a 6-31G basis set,[35] the dangling bonds were passivated with hydrogen atoms, and the positions of the hydrogen atoms were optimized at the B3LYP/6-31G level of theory.[35−37] Chemical shieldings and NICS were calculated at the B3LYP/6-311G level of theory[38] for the resulting flat circumcoronene structure and were used for comparison.

The reported radius of curvature of the nanotubes was calculated using the following formula:[39]

$$r = \frac{a[3(n^2 + nm + m^2)]^{0.5}}{2\pi}$$

where a = 1.42 Å.

RESULTS AND DISCUSSION

Table 1 lists calculated shielding values for several flat and curved aromatic structures. Many of these values have been calculated before and are available in the literature,[11,12,19] but since many of these calculations were done with different computational methods, we list our values here for consistency. Another reason for presenting these values in Table 1 is to show that our calculations have some relevance to experiments and to verify that the level of theory we have chosen is sufficient for our purposes. In Figure 3 we compare experimental chemical shifts available in the literature with our calculated shielding for these compounds. The agreement is quite good, allowing us to continue to the discussion of chemical shielding in our 54-carbon model curved structures.

We first consider the change in the isotropic shielding of the central carbon atoms as curvature is introduced in a

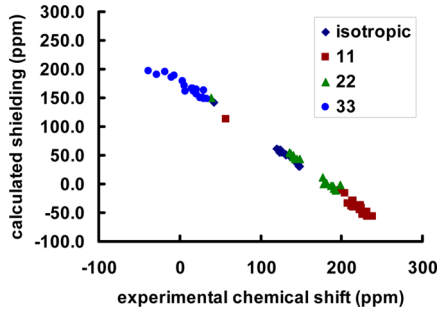

Figure 3. Comparison of experimental chemical shift and calculated chemical shieldings tensor components for several flat and curved compounds (data in Table 1). The data can be fit with a linear regression line having a slope of −0.98 and R^2 of 0.99.

circumcoronene-like system. Figure 4 shows the differences in isotropic shielding between the curved and flat 54-carbon

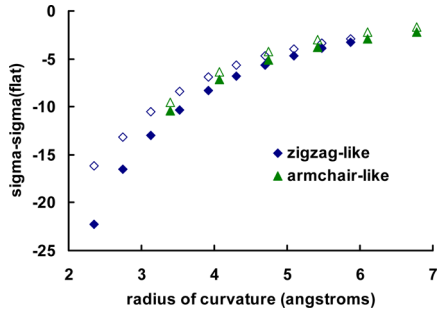

Figure 4. Isotropic chemical shielding of "zigzag-like" and "armchair-like" curved circumcoronene analogs, compared to the isotropic shielding of flat circumcoronene. Filled markers are for the four carbons that remain coplanar as the structure is curved and open markers represent the two carbons that do not remain coplanar.

DOI: 10.1021/acs.jpca.6b05560
J. Phys. Chem. A 2016, 120, 7011−7019

structure as a function of the radius of curvature. Introducing curvature leads to a decrease in isotropic shielding of the central carbon atoms, and this decrease becomes more pronounced as the radius of curvature decreases. We introduced curvature along two mutually perpendicular directions, labeled as the x and y directions in Figure 1d, by cutting the 54-carbon fragments from zigzag and armchair nanotubes, respectively. We term these two sets of curved fragments "zigzag-like" and "armchair-like" to denote the different directions of curvature. As can be seen from Figure 4, introducing curvature along the two perpendicular directions leads to a similar change in isotropic chemical shielding. In both cases, the isotropic shielding values approach the value of the flat structure as the radius of curvature is increased.

When curvature is introduced in either the zigzag-like or armchair-like directions, the six atoms in the central aromatic ring do not remain coplanar. Instead, four carbons remain coplanar and the other two are pulled out of the plane due to the curvature. Thus, we have presented the average shielding value for the four coplanar atoms (filled markers in Figure 4) as well as the average value for the two remaining atoms (open markers in Figure 4). The latter value is always more shielded, and, as expected, as the radius of curvature decreases the difference in chemical shielding between the four coplanar atoms and the two remaining atoms becomes more pronounced as the degree of nonplanarity increases. The difference in shielding between the four coplanar atoms and the two remaining carbon atoms in the central aromatic ring is greater in the zigzag-like structure than in the armchair-like structure because the degree of noncoplanarity of these atoms is greater in the zigzag-like structures (introducing curvature along the x direction in Figure 1d pulls these two atoms out of the plane more than does introducing curvature along the y direction).

In addition to the isotropic shielding, we also examined how introducing curvature influences the principal components of the chemical shielding tensor. The three principal components of the chemical shielding tensor for each structure are listed in Table 2. The shielding tensor orientation is similar to that of polycyclic aromatic hydrocarbons. For a flat aromatic structure, the σ_{11} and σ_{22} components lie in the plane of the aromatic ring, while σ_{33} is perpendicular to the plane of the ring. For our curved structures, the σ_{33} component is oriented radial to the curve. In Figure 5, the difference in shielding of each principal component between the flat and curved structure is plotted as a function of the radius of curvature. Introducing curvature leads to a decrease in shielding for all three tensor components, with the σ_{33} component having the largest change. A decrease in shielding, as indicated by a downfield shift in the δ_{33} component of carbon chemical shift tensors, has been observed in other curved structures, and has been attributed to the σ_{33} component in flat structures being influenced primarily by σ electron density, while the curvature causes this component to be influenced by π electron density as well.[13,12]

In addition to the three principal components, σ_{11}, σ_{22}, and σ_{33}, the shielding tensor can also be described by a span and a skew.[40,41] The span of a shielding tensor, Ω, is defined as the difference between the most shielded and least shielded principal components:

$$\Omega = \sigma_{33} - \sigma_{11}$$

The span is therefore a measure of the width of the shielding tensor. The skew, κ, is defined as

Table 2. Chemical Shielding Tensor Components in Curved Structures (ppm)[a]

zigzag-like						
radius of curvature	$\sigma(11)$		$\sigma(22)$		$\sigma(33)$	
2.35	−24.5	−14.2	−9.5	−10.9	167.0	175.8
2.74	−18.9	−12.0	−7.4	−9.7	176.3	181.5
3.13	−14.7	−9.8	−5.6	−7.4	181.0	185.1
3.52	−11.8	−8.2	−4.2	−5.6	184.7	187.9
3.91	−9.7	−7.1	−3.2	−4.3	187.6	190.1
4.31	−8.2	−6.2	−2.2	−3.2	189.7	191.8
4.70	−7.0	−5.6	−1.5	−2.4	191.3	193.1
5.09	−6.1	−5.2	−0.9	−1.7	192.7	194.2
5.48	−5.4	−4.7	−0.3	−1.2	193.8	195.1
5.87	−4.9	−4.4	0.1	−0.8	194.7	195.7
(flat)	−2.1	−2.3	1.7	1.8	200.1	199.7
armchair-like						
radius of curvature	$\sigma(11)$		$\sigma(22)$		$\sigma(33)$	
3.39	−10.3	−11.2	−5.7	−3.6	184.6	185.4
4.07	−7.7	−8.1	−3.4	−1.7	189.2	190.0
4.75	−6.1	−6.2	−1.9	−0.5	192.3	193.1
5.42	−5.2	−5.1	−1.0	0.2	194.5	195.2
6.10	−4.6	−4.5	−0.5	0.6	196.0	196.6
6.78	−4.2	−4.0	0.0	0.8	197.1	197.5
(flat)	−2.1	−2.3	1.7	1.8	200.1	199.7

[a]For each principal component, the first number is for the four carbons that remain coplanar, and the second number is for the two carbons that do not remain in the plane.

$$\kappa = 3(\sigma_{iso} - \sigma_{22})/(\sigma_{33} - \sigma_{11})$$

where σ_{iso} is the isotropic chemical shielding. The skew thus ranges from +1 (when $\sigma_{11} = \sigma_{22}$) to −1 (when $\sigma_{22} = \sigma_{33}$). A skew of zero occurs when σ_{22} is midway between σ_{11} and σ_{33} (i.e., $\sigma_{22} = \sigma_{iso}$).[41]

The span and skew of the carbon shielding tensors for the curved structures are plotted in Figure 6. Filled and open markers represent the four carbons remaining coplanar and the two remaining carbons in the central ring, respectively, and the average span and skew for the six central carbons in a flat circumcoronene structure are indicated by a dashed line. Since all principal components are less shielded as the radius of curvature decreases, and since σ_{33}, the most shielded component, decreases the most, increasing curvature also leads to a decrease in the span of the shielding tensor. As the radius of curvature increases, the span approaches the value of carbons in the flat structure.

The skew of the shielding tensor for all structures is close to +1, meaning that the shielding tensor is nearly axially symmetric with $\sigma_{11} \approx \sigma_{22}$. This is a result of the electronic environment surrounding each carbon being nearly isotropic in the plane of the central carbon ring. For the armchair-like structures, introducing curvature leads to only a slight decrease in the skew (from 0.96 to 0.92) indicating that the difference between the σ_{11} and σ_{22} chemical shielding tensor components remains small for both the carbons that remain coplanar and those that do not. In the case of the zigzag-like structures, the tensor deviates slightly from axial symmetry (to a skew of 0.84 for the most curved structure) for the four carbons that remain coplanar, whereas the skew increases slightly to 0.98 for the two carbons that do not remain coplanar when curvature is introduced. Introducing curvature into the circumcoronene molecule therefore does not lead to a large deviation from axial

DOI: 10.1021/acs.jpca.6b05560
J. Phys. Chem. A 2016, 120, 7011−7019

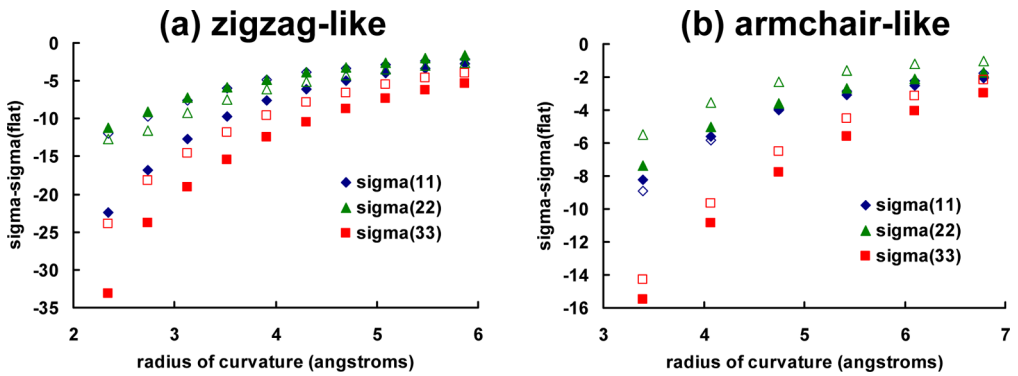

Figure 5. Chemical shielding tensor components in the curved structures, compared to the analogous chemical shielding component in flat circumcoronene; (a) zigzag-like structures and (b) armchair-like structures. Filled markers are for the four carbons that remain coplanar as the structure is curved, and open markers represent the two carbons that do not remain coplanar.

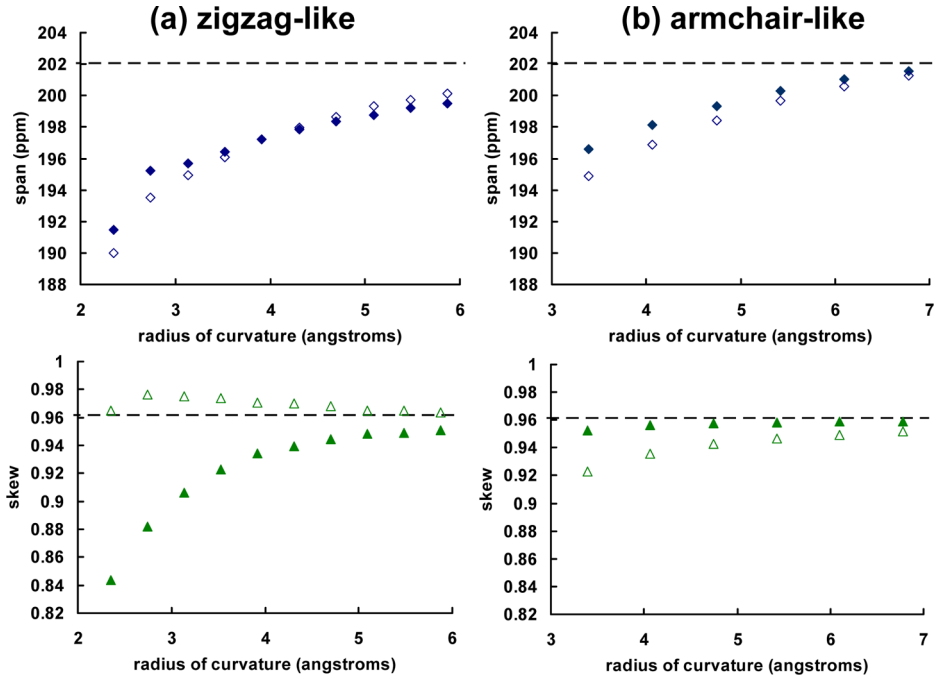

Figure 6. Span and skew of the carbon chemical shielding tensor as a function of curvature; (a) zigzag-like structures and (b) armchair-like structures. Filled markers are for the four carbons that remain coplanar as the structure is curved and open markers represent the two carbons that do not remain coplanar. The corresponding span and skew for flat circumcoronene are indicated by a dashed line.

Table 3. Experimental and Calculated Chemical Shift Tensor Components in Pyrene and 1,8-Dioxa[8](2,7)pyrenophane (ppm)

	experimental[a]			calculations[a] (lit.)			calculations (this work)		
	$\delta(11)$	$\delta(22)$	$\delta(33)$	$\delta(11)$	$\delta(22)$	$\delta(33)$	$\sigma(11)$	$\sigma(22)$	$\sigma(33)$
pyrene	197.0	191.0	−18.0				−12.0	−7.9	195.8
pyreneophane	211.9	171.6	0.8	202.8	190.8	−6.0	−19.9	−8.6	193.3
curved pyrene							−30.4	−13.8	186.4
curved OH							−24.3	−9.8	185.7
curved OCH_3							−24.5	−9.2	185.2

[a]Data from ref 13.

symmetry of the chemical shielding tensor for carbons in the central aromatic ring.

Calculated chemical shielding values of pyrene carbons in the 1,8-dioxa[8](2,7)pyrenophane molecule, for which experimental chemical shifts are available,[13] follow the same trends. Table 3 compares experimental and calculated chemical shift tensor elements and calculated chemical shielding tensor elements for 1,8-dioxa[8](2,7)pyrenophane, as well as for pyrene, the analogous flat structure. Our calculated shielding values indicate that all three components of the chemical shielding tensor are less shielded in the curved pyreneophane than in the flat pyrene molecule, with σ_{22} having the smallest change. However, the experimental values suggest a ∼ 20 ppm increase in shielding of δ_{22} going from the flat pyrene molecule to the curved 1,8-

DOI: 10.1021/acs.jpca.6b05560
J. Phys. Chem. A 2016, 120, 7011−7019

dioxa[8](2,7)pyrenophane molecule. Chemical shifts that have been calculated[13] using a larger basis set (Pyreneophane heavy atom coordinates were taken from the crystal structure and the hydrogen atom positions were optimized using B3LYP/6-311G**. Chemical shieldings were also calculated using B3LYP/6-311G**) also do not well reproduce the experimental value of δ_{22} for the curved 1,8-dioxa[8](2,7)-pyrenophane. Calculations for a curved pyrene molecule with carbon atoms placed at the coordinates of the corresponding carbon atoms in the pyreneophane crystal structure, as well as calculations for a curved pyrene with −OH and methoxy substituents (listed in the last three rows of Table 3) indicate that this large discrepancy between calculated and experimental values of the δ_{22} component is not due to substituent effects.

NICSs are important not only as a measure of aromaticity but as an indicator of the change in chemical shift that would be felt by a nucleus located at a particular position in space, due to ring current effects from nearby aromatic rings. Since it is related to the aromaticity of a molecule, the NICS is expected to be influenced by the circulating current density in aromatic compounds. In Figure 7, we show the isotropic values of NICS

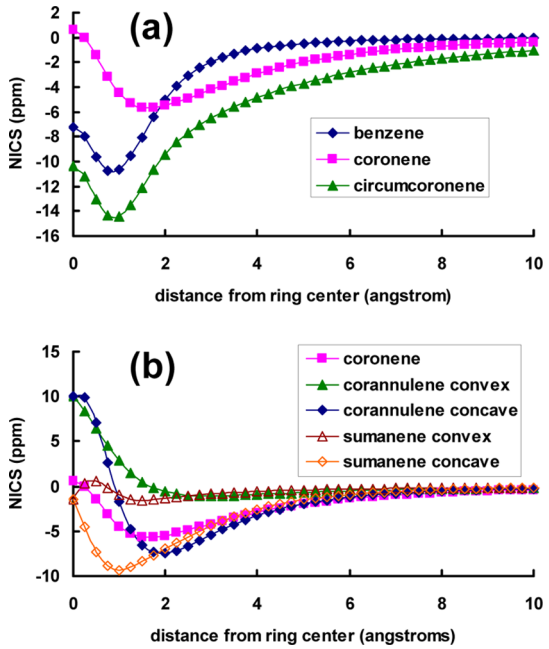

Figure 7. NICSs calculated on a line normal to the plane containing the central carbon ring as a function of distance from the center of the ring for a selection of (a) flat and (b) curved molecules. NICS for coronene are also included in (b) for comparison.

calculated along a line normal to the central carbon ring in several flat (Figure 7a) and curved (Figure 7b) aromatic structures. These values are in good agreement with those in the literature.[2,28,42] The NICS values in the center of the central aromatic ring (NICS(0), 0 on the abscissa in Figure 7) for benzene, coronene, circumcoronene, and corannulene are in agreement with the calculated current densities for these molecules.[16,17] Benzene and circumcoronene have diatropic ring currents in their central aromatic ring, and have negative NICS(0) values. On the other hand, coronene and corannulene[43] have paratropic ring currents in their central aromatic ring and have positive NICS(0) values. As can be seen in Figure 7a, benzene and circumcoronene have a maximum (highest magnitude) NICS at about 1.0 Å from the center of the ring, while coronene, also a flat molecule, has a maximum NICS closer to 1.75 Å from the ring.

Figure 7b illustrates the difficulty in comparing flat and curved structures with different numbers of carbon atoms and with different numbers of five- and six-membered rings. NICS calculated on a line normal to the central carbon ring of coronene, a flat molecule, are shown for comparison with the NICS calculated on the concave and convex sides of the curved molecules corannulene and sumanene. As can be seen from Figure 7b, there is no clear relationship between either the maximum NICS value or the distance of the maximum NICS from the ring center and the curvature of the system. For this reason, we aimed to compare NICS on the concave and convex faces of curved molecules with different degrees of curvature, but the same number of carbon atoms and aromatic rings.

For each of our curved circumcoronene-like structures, NICSs were calculated on a line perpendicular to the central carbon ring on the convex and concave side of each structure, and are shown in Figure 8. For reference, the NICS for a flat circumcoronene molecule is also shown in red on each graph. In all cases, the NICS is everywhere negative (meaning that a nucleus placed near either face of the structures feels a shielding effect) and approaches zero as the distance from the ring center increases. Since the NICS are always negative, in the rest of this paragraph we will refer to the magnitude of the NICS. The maximum NICS (largest magnitude) occurs at about 1 Å from the face of the aromatic ring. For both the zigzag-like and armchair-like structures, the NICS decreases on the convex side and increases on the concave side as the radius of curvature decreases. Notably, the decrease of the NICS on the convex side is greater than the increase on the concave side. We attribute this to two competing factors. As the radius of curvature decreases and the degree of curvature increases, the aromaticity of the central carbon ring is presumably destroyed due to a decrease in orbital overlap as the geometry is distorted from flat. This would be expected to lead to a decrease in NICS for both the convex and concave side. However, as the degree of curvature increases, geometrical effects are also present. Increasing the curvature brings the outer aromatic rings closer to the concave face of the central aromatic ring. This increases the NICS on the concave side of the structure, since a nucleus placed near this face now feels ring current effects not only from the central aromatic ring, but also stronger ring currents from the outer aromatic rings. The competing effects of decreasing aromaticity and the outer rings moving closer to the concave face as curvature increases leads to a negligible difference in NICS among the curved structures (some anomalies in the NICS values for the concave side between 2 and 4 Å are due to the influence of the protons and carbons on the "other side" of the curved structure).

The change in NICS with curvature can perhaps be seen more clearly in Figure 9, which plots the NICS at the ring center (called NICS(0)), the NICS 1 Å from the ring center on the convex face (NICS(1)), and the NICS 1 Å from the ring center on the concave face (NICS(−1)) compared to the corresponding NICS for the flat structure. The open data points are for the zigzag-like structures and the filled data points are for the armchair-like structures. For both zigzag-like and armchair-like structures, the NICS(0) becomes slightly more positive upon increasing curvature, meaning that the magnitude of the shielding effect induced by the structure decreases. The difference between the NICS(0) in the zigzag-like and

DOI: 10.1021/acs.jpca.6b05560
J. Phys. Chem. A 2016, 120, 7011−7019

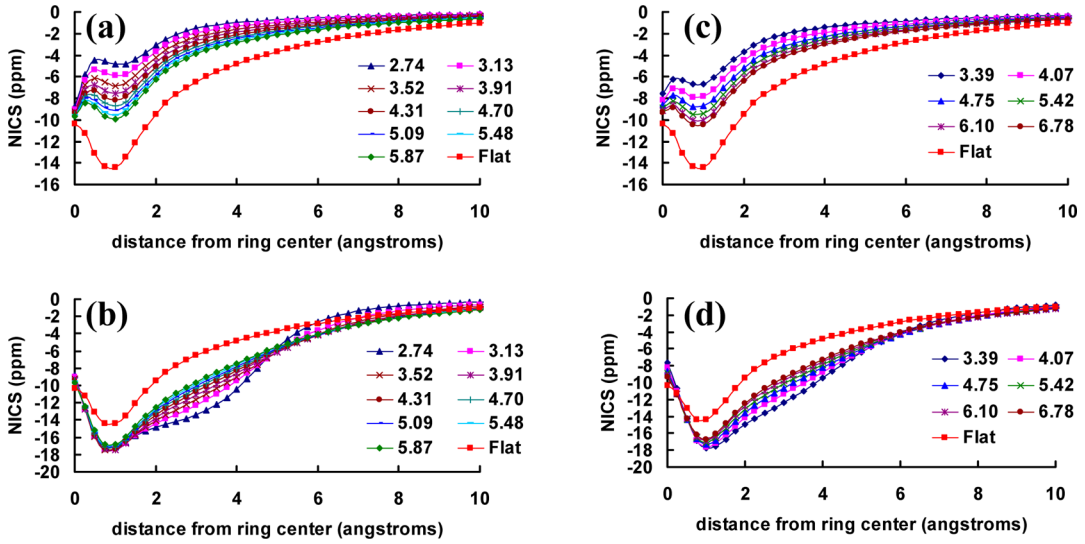

Figure 8. NICSs as a function of distance from the ring center; (a) on the convex side of zigzag-like structures, (b) on the concave side of zigzag-like structures, (c) on the convex side of armchair-like structures, and (d) on the concave side of armchair-like structures. The radius of curvature of each curved structure is indicated, and the corresponding NICS for the flat circumcoronene structure is shown in red for comparison.

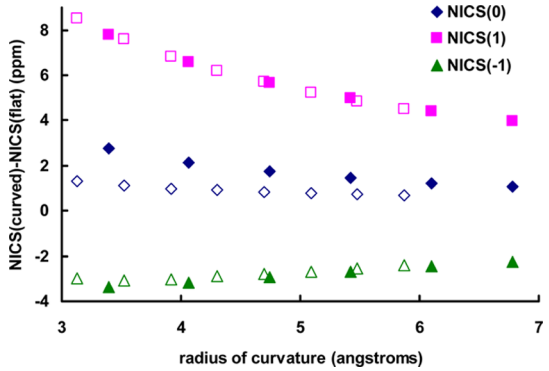

Figure 9. Change in NICS as a function of curvature, as compared to the flat structure. Values shown are NICS for the curved structure minus NICS for the flat structure, so that a negative number means that the NICS is more shielded in the curved than in the corresponding flat structure. NICS were measured at the center of the central aromatic ring (NICS(0)) and 1 Å above (convex face, NICS(1)) or below (concave face, NICS(−1)) the plane of the central aromatic ring. Filled points are for the armchair-like structures and open points are for the zigzag-like structures.

armchair-like structures can be due to the method used to define the center of the aromatic ring, since only the four carbons that remain coplanar in each structure were used to calculate the geometric ring center. For the NICS(1) and NICS(−1), the agreement between the zigzag-like and armchair-like structures is better. Increasing curvature causes the NICS(1) on the convex face to increase and the NICS(−1) on the concave face to decrease, but the effect is greater for the NICS(1) due to cancellation from competing effects of decreasing aromaticity and outer rings being brought closer to the concave face. In Figure 9, highly curved structures with a radius of curvature less than 3 Å were not considered since the NICS(1) and NICS(−1) in these structures are influenced by atoms on the other side of the curved structure.

CONCLUSIONS

The change in chemical shielding of carbons in curved polycyclic aromatic hydrocarbons has been systematically studied by examining curved structures with the same number of carbon atoms as the flat circumcoronene molecule. We found that increasing the degree of curvature (decreasing the radius of curvature) leads to a monotonic decrease in shielding, with the σ_{33} component having the largest change. Introducing curvature in either the x or y direction, corresponding to armchair-like or zigzag-like structures, has a similar effect on the resulting shielding values. The span of the chemical shielding tensor decreases as the degree of curvature is increased, while the skew remains close to +1, indicating that the electronic environments in the directions of the σ_{11} and σ_{22} shielding tensor components are similar.

In addition, increasing the curvature causes the NICS on the concave side of the curved structure to increase in magnitude and the NICS on the convex side to decrease in magnitude. However, the same radius of curvature has a greater effect on the NICS on the concave side than on the convex side. We believe this is due to two competing factors. As the curvature increases, aromaticity of the central ring is destroyed, leading to a decrease in magnitude of the NICS. However, as the curvature increases, points on the concave side are also brought into closer proximity to the faces of other rings, leading to an increase in shielding. This increase in shielding outweighs the decrease due to loss of aromaticity, but as both factors are contributing, the shielding increase is not as great on the concave side as the shielding decrease on the convex side. The work described here will be important in understanding experimental carbon chemical shifts in curved systems such as carbon nanotubes, fullerenes, and similar structures.

AUTHOR INFORMATION

Corresponding Author

*E-mail: lcasabi@clemson.edu.

Notes

The author declares no competing financial interest.

DOI: 10.1021/acs.jpca.6b05560
J. Phys. Chem. A 2016, 120, 7011−7019

■ ACKNOWLEDGMENTS

This work was made possible by computing time on Clemson University's Palmetto computing cluster. The author would like to thank Prof. Angel C. de Dios (Georgetown University) for his valuable comments on the manuscript.

■ REFERENCES

(1) Scott, L. T. Chemistry at the Interior Atoms of Polycyclic Aromatic Hydrocarbons. *Chem. Soc. Rev.* **2015**, *44*, 6464.
(2) Forse, A. C.; Griffin, J. M.; Presser, V.; Gogotsi, Y.; Grey, C. P. Ring Current Effects: Factors Affecting the NMR Chemical Shift of Molecules Adsorbed on Porous Carbons. *J. Phys. Chem. C* **2014**, *118*, 7508−7514.
(3) Harris, P. J. F.; Tsang, S. C. High-Resolution Electron Microscopy Studies of Non-Graphitizing Carbons. *Philos. Mag. A* **1997**, *76*, 667−677.
(4) Harris, P. J. F. Structure of Non-Graphitising Carbons. *Int. Mater. Rev.* **1997**, *42*, 206−218.
(5) Heister, E.; Brunner, E. W.; Dieckmann, G. R.; Jurewicz, I.; Dalton, A. B. Are Carbon Nanotubes a Natural Solution? Applications in Biology and Medicine. *ACS Appl. Mater. Interfaces* **2013**, *5*, 1870−1891.
(6) Endo, M.; Strano, M. S.; Ajayan, P. M. Potential applications of carbon nanotubes. In *Carbon Nanotubes: Advanced Topics in the Synthesis, Structure, Properties and Applications*; Jorio, A., Dresselhaus, G., Dresselhaus, M. S., Eds.; Springer: Berlin, 2008; pp 13−61.
(7) Scott, L. T.; Cheng, P.-C.; Hashemi, M. M.; Bratcher, M. S.; Meyer, D. T.; Warren, H. B. Corannulene. A Three-Step Synthesis. *J. Am. Chem. Soc.* **1997**, *119*, 10963.
(8) Sakurai, H.; Daiko, T.; Hirao, T. A Synthesis of Sumanene, a Fullerene Fragment. *Science* **2003**, *301*, 1878.
(9) Iijima, S. Helical Microtubules of Graphitic Carbon. *Nature* **1991**, *354*, 56−58.
(10) Cresti, A.; Nemec, N.; Biel, B.; Niebler, G.; Triozon, F.; Cuniberti, G.; Roche, S. Charge Transport in Disordered Graphene-Based Low Dimensional Materials. *Nano Res.* **2008**, *1*, 361−394.
(11) Orendt, A. M.; Facelli, J. C.; Bai, S.; Rai, A.; Gossett, M.; Scott, L. T.; Boerio-Goates, J.; Pugmire, R. J.; Grant, D. M. Carbon-13 Shift Tensors in Polycyclic Aromatic Compounds. 8. A Low-Temperature NMR Study of Coronene and Corannulene. *J. Phys. Chem. A* **2000**, *104*, 149−155.
(12) Halling, M. D.; Orendt, A. M.; Strohmeier, M.; Solum, M. S.; Tsefrikas, V. M.; Hirao, T.; Scott, L. T.; Pugmire, R. J.; Grant, D. M. Solid-State ^{13}C NMR Investigations of 4,7-dihydro-1H-tricyclopenta-[*def,jkl,pqr*]triphenylene (Sumanene) and indeno[1,2,3-*cd*]-fluoranthene: Buckminsterfullerene Moieties. *Phys. Chem. Chem. Phys.* **2010**, *12*, 7934−7941.
(13) Halling, M. D.; Sagar Unikela, K.; Bodwell, G. J.; Grant, D. M.; Pugmire, R. J. Solid-State ^{13}C NMR Investigations of Cyclophanes: [2.2]Paracyclophane and 1,8-Dioxa[8](2,7)pyrenophane. *J. Phys. Chem. A* **2012**, *116*, 5193−5198.
(14) Tycko, R.; Haddon, R. C.; Dabbagh, G.; Glarum, S. H.; Douglass, D. C.; Mujsce, A. M. Solid-State Magnetic Resonance Spectroscopy of Fullerenes. *J. Phys. Chem.* **1991**, *95*, 518−520.
(15) Yannoni, C. S.; Johnson, R. D.; Meijer, G.; Bethune, S.; Salem, J. R. Carbon-13 NMR Study of the C_{60} Cluster in the Solid-State − Molecular Motion and Carbon Chemical Shift Anisotropy. *J. Phys. Chem.* **1991**, *95*, 9−10.
(16) Steiner, E.; Fowler, P. W. Patterns of Ring Currents in Conjugated Molecules: A Few-Electron Model Based on Orbital Contributions. *J. Phys. Chem. A* **2001**, *105*, 9553−9562.
(17) Soncini, A.; Steiner, E.; Fowler, P. W.; Havenith, R. W. A.; Jenneskens, L. W. Perimeter Effects on Ring Currents in Polycyclic Aromatic Hydrocarbons: Circumcoronene and Two Hexabenzocoronenes. *Chem. - Eur. J.* **2003**, *9*, 2974−2981.
(18) Martín-Martínez, F. J.; Melchor, S.; Dobado, J. A. Edge Effects, Electronic Arrangement, and Aromaticity Patterns on Finite-Length Carbon Nanotubes. *Phys. Chem. Chem. Phys.* **2011**, *13*, 12844−12857.
(19) Carter, C. M.; Alderman, D. W.; Facelli, J. C.; Grant, D. M. Carbon-13 Chemical Shielding Tensors in Polycyclic Aromatic Compounds.1. Single-Crystal Study of Pyrene. *J. Am. Chem. Soc.* **1987**, *109*, 2639−2644.
(20) Schleyer, P. v. R.; Maeker, C.; Dransfeld, A.; Jiao, H.; Hommes, N. J. R. v. E. Nucleus-Independent Chemical Shifts: A Simple and Efficient Aromaticity Probe. *J. Am. Chem. Soc.* **1996**, *118*, 6317−6318.
(21) Wolinski, K. Magnetic Shielding Surface in Molecules. Neutron as a Probe in the Hypothetical Magnetic Resonance Spectroscopy. *J. Chem. Phys.* **1997**, *106*, 6061−6067.
(22) Subramanian, G.; Schleyer, P. v. R.; Jiao, H. Are the Most Stable Fused Heterobicycles the Most Aromatic? *Angew. Chem., Int. Ed. Engl.* **1996**, *35*, 2638−2641.
(23) Lazzeretti, P. Assessment of Aromaticity via Molecular Response Properties. *Phys. Chem. Chem. Phys.* **2004**, *6*, 217−223.
(24) Miyake, N.; Yamaki, D.; Hada, M. Magnetic Shielding in Carbon Nanotube. *AIP Conf. Proc.* **2009**, *1504*, 856−859.
(25) Aghamohammadi, M.; Shahdousti, P.; Ghafouri, R.; Anafcheh, M. Exploring Magnetic Properties and Curved Pi-Conjugation of BxNyCz Nanotubes using Density Functional Theory. *Superlattices Microstruct.* **2013**, *57*, 66−76.
(26) Kibalchenko, M.; Payne, M. C.; Yates, J. R. Magnetic Response of Single-Walled Carbon Nanotubes Induced by an External Magnetic Field. *ACS Nano* **2011**, *5*, 537−545.
(27) Ferrer, S. M.; Molina, J. M. Theoretical Calculations on $C_{30}H_{12}$ Bowl-Shaped Hydrocarbons: NMR Shielding Constants, Stability, and Aromaticity. *J. Comput. Chem.* **1999**, *20*, 1412−1421.
(28) Reisi-Vanani, A.; Rezaei, A. A. Evaluation of the Aromaticity of Non-Planar and Bowl-Shaped Molecules by NICS Criterion. *J. Mol. Graphics Modell.* **2015**, *61*, 85−88.
(29) Zurek, E.; Pickard, C. J.; Walczak, B.; Autschbach, J. Density Functional Study of the ^{13}C NMR Chemical Shifts in Small-to-Medium-Diameter Infinite Single-Walled Carbon Nanotubes. *J. Phys. Chem. A* **2006**, *110*, 11995−12004.
(30) Humphrey, W.; Dalke, A.; Schulten, K. VMD - Visual Molecular Dynamics. *J. Mol. Graphics* **1996**, *14*, 33−38. http://www.ks.uiuc.edu/Research/vmd/. Date last accessed: 16 August 2016.10.1016/0263-7855(96)00018-5
(31) Frisch, M. J.; et al. Gaussian 09, Revision D.01; Gaussian, Inc.: Wallingford, CT, 2009.
(32) Henderson, T. M.; Izamaylov, A. F.; Scalmani, G.; Scuseria, G. E. Can Short-Range Hybrids Describe Long-Range-Dependent Properties? *J. Chem. Phys.* **2009**, *131*, 044108.
(33) Heyd, J.; Scuseria, G. E.; Ernzerhof, M. Erratum: "Hybrid Functionals Based on a Screened Coulomb Potential" [J. Chem. Phys.118, 8207 (2003)]. *J. Chem. Phys.* **2006**, *124*, 219906.
(34) Heyd, J.; Scuseria, G. E.; Ernzerhof, M. Hybrid Functionals Based on a Screened Coulomb Potential. *J. Chem. Phys.* **2003**, *118*, 8207.
(35) Hehre, W. J.; Ditchfield, R.; Pople, J. A. Self—Consistent Molecular Orbital Methods. XII. Further Extensions of Gaussian—Type Basis Sets for Use in Molecular Orbital Studies of Organic Molecules. *J. Chem. Phys.* **1972**, *56*, 2257.
(36) Becke, A. D. Density-Functional Thermochemistry. III. The Role of Exact Exchange. *J. Chem. Phys.* **1993**, *98*, 5648.
(37) Lee, C.; Yang, W.; Parr, R. G. Development of the Colle-Salvetti Correlation-Energy Formula into a Functional of the Electron Density. *Phys. Rev. B: Condens. Matter Mater. Phys.* **1988**, *37*, 785.
(38) Krishnan, R.; Binkley, J. S.; Seeger, R.; Pople, J. A. Self-Consistent Molecular Orbital Methods. XX. A Basis Set for Correlated Wave Functions. *J. Chem. Phys.* **1980**, *72*, 650.
(39) Sun, S.; Kürti, J.; Kertesz, M.; Baughman, R. H. Variations of the Geometries and Band Gaps of Single-Walled Carbon Nanotubes and the Effect of Charge Injection. *J. Phys. Chem. B* **2003**, *107*, 6924−6931.
(40) Jameson, C. J. Reply to 'Conventions for Tensor Quantities Used in Nuclear Magnetic Resonance, Nuclear Quadrupole Resonance and Electron Spin Resonance Spectroscopy'. *Solid State Nucl. Magn. Reson.* **1998**, *11*, 265−268.

DOI: 10.1021/acs.jpca.6b05560
J. Phys. Chem. A 2016, 120, 7011−7019

(41) Mason, J. Conventions for the Reporting of Nuclear Magnetic Shielding (or Shift) Tensors Suggested by Participants in the NATO ARW on NMR Shielding Constants at the University of Maryland, College Park, July 1992. *Solid State Nucl. Magn. Reson.* **1993**, *2*, 285−288.
(42) Forse, A. C.; Merlet, C.; Allan, P. K.; Humphreys, E. K.; Griffin, J. M.; Aslan, M.; Zeiger, M.; Presser, V.; Gogotsi, Y.; Grey, C. P. New Insights into the Structure of Nanoporous Carbons from NMR, Raman, and Pair Distribution Function Analysis. *Chem. Mater.* **2015**, *27*, 6848−6857.
(43) Steiner, E.; Fowler, P. W.; Jenneskens, L. W. Counter-Rotating Ring Currents in Coronene and Corannulene. *Angew. Chem., Int. Ed.* **2001**, *40*, 362−366.

DOI: 10.1021/acs.jpca.6b05560
J. Phys. Chem. A 2016, 120, 7011−7019